Desalination and Water Treatment
www.deswater.com

doi:10.5004/dwt.2018.22727

124 (2018) 256–266
August

Degrading quinoline wastewater by catalytic wet peroxide oxidation

Zhaojie Jiao[a,b], Guilin Zhou[b], Haidong Zhang[b], Yu Shen[b], Xianming Zhang[b], Xu Gao[a,c,*]

[a]*Faculty of Urban Construction and Environmental Engineering, Chongqing University, Chongqing 400045, China, Tel./Fax +86-23-62768317, email: Jiaozhaojie2001@163.com (Z. Jiao)*
[b]*Engineering Research Center for Waste Oil Recovery Technology and Equipment of Ministry of Education, Chongqing Technology and Business University, Chongqing 400067, China, Tel./Fax +86-23-62768316, email: dicpglzhou@ctbu.edu.cn (G. Zhou), Tel./Fax +86-23-62768316, email: haidongzhang@ctbu.edu.cn (H. Zhang), Tel./Fax +86-23-62768316, email: shenyu@ctbu.edu.cn (Y. Shen), Tel./Fax +86-23-62768316, email: zxm215@126.com (X. Zhang)*
[c]*Chongqing Water Group Company Limited, Chongqing 400015, China, Tel./Fax +86-23-62768317, email: gaoxu@cqu.edu.cn (X. Gao)*

Received 5 September 2017; Accepted 12 July 2018

ABSTRACT

This research aimed to degrade quinoline wastewater using CWPO (short for catalytic wet peroxide oxidation). Following the complexation method Cu-Ce composite oxide catalysts were prepared. The properties of catalysts were characterized by probed into by employing XRD (short for X-ray diffraction), SEM (short for scanning electron microscopy), H_2-TPR (short for temperature programmed reduction) and XPS (short for X-ray photoelectron spectroscopy). Also, the degradation properties of varying Cu/Ce molar ratios, catalysts and H_2O_2 dosages and the initial pH of solution were investigated in the degrading of simulated quinoline wastewater. As the research results suggested, CeO_2 and CuO for the prepared Cu-Ce composite oxide catalyst will become a Cu-Ce-O solid solution under calcination at high temperature, taking on a loose and porous structure on the surface. A little surface Cu_2O will often appear as well though CeO_2 and CuO are the main substances on the surface. The lattice oxygen on the surface is greater than the adsorbed oxygen and hydroxyl oxygen in amount; thus, the phase structure of this oxygen is greatly impacted by the Cu/Ce molar ratio. Besides, its reducibility decreases as Cu content increases. The Cu-Ce composite oxide catalyst takes on a potent performance of catalytic wet peroxide oxidation for simulated quinoline wastewater. The catalyst degradation performance turns the optimal under initial quinoline concentration of 100 mg L^{-1}, Cu/Ce molar ratio of 1.0, dosage of catalyst and H_2O_2 of 0.16 g L^{-1} and 196 mmol L^{-1}, respectively. Under these conditions, the TOC removal can reach 91.1%. The catalyst is highly adapted to pH. The removal efficiency of quinoline can be actually high under the pH value ranging from 5.1 and 10.5, and its reaction follows the first-order reaction kinetics equation.

Keywords: Catalytic wet peroxide oxidation (CWPO); Quinoline wastewater; Cu-Ce mixed oxide catalyst; TOC removal

1. Introduction

Quinoline counts as a typical nitrogen-containing heterocyclic compound, applied in several industries, inclusive of processing food, rubber, pharmaceuticals, synthetic dyes, pesticides and refined oil [1,2]. Quinoline and its derivatives are high in water solubility and able to transfer the surface water to the water environment. Because of its volatile properties, it can also be found in urban air and tobacco smoke. This type of compound is a comparatively stable in ring structure, and difficult to biodegrade. It accumulates rapidly in natural water sources, restraining the growth of animals and plants and exerting carcinogenic, teratogenic and mutagenic effects [3,4]. Such substances fail to be readily degraded following the traditional activated

*Corresponding author.

sludge method. Some researches [5,6] have degraded quinoline wastewater using efficient bacteria, whereas it was comparatively time-consuming. Besides, 2-hydroxyquinoline, the primary degradation products of Quinoline, can also overall inhibit degradation [7]. The amount of quinoline in oily wastewater and cooking wastewater has been reported as nearly 0.1% [8] and 5% [9], respectively, of the total mass fraction of detected contaminants after biochemical treatment. Accordingly, it is crucial to find the best way to treat Quinoline-contaminated wastewater for the wastewater remediation industries.

Advanced oxidation techniques focused on producing free oxyradicals have been developed in recent years, primarily targeting at the treatment of degradation-resistant organic wastewater, e.g. quinoline. Supercritical water oxidation [10], ozone oxidation [11], ultraviolet radiation [12], photocatalytic oxidation [13], electrocatalytic oxidation [14], wet oxidation [15] and others are provided by the mentioned advanced oxidation techniques. Advanced oxidation technique is advantaged in potent oxidation capacity for quinoline and other refractory organic matters. Such technique has become highly used in the field of water treatment as able to oxidize the refractory organic matter into carbon dioxide and water at a fast reaction rate.

CWPO serves as a wastewater treatment technique developed on CWO (short for catalytic wet oxidation). Heterogeneous catalysts can catalyze and decompose H_2O_2 into highly oxidant ·OH under CWPO technique [16]. This technique has tackled down corrosion of equipment, safety in operation, and high operating costs caused by the high pressure in wet oxidation by virtue of the low reaction temperature and pressure. Besides, H_2O_2 other than gas oxidants is employed, avoiding the gas-liquid mass transfer resistance, thus accelerating the reaction. As a result, the loss of active components in catalysts, failure in their repeated use, secondary pollution and etc. are addressed [17].

The stability of the catalyst counts as one of the key factors affecting CWPO technique. Numerous researches have been performed in recent years, incorporating rare earth elements to increase the stability of catalysts, especially the rare earth element cerium (Ce) [18,19], which is a good electronic additive capable of promoting the oxygen transfer [20]. Cerium oxide takes on potent oxygen storage performance and can increase catalyst activity and selectivity [21], thus providing a stable crystal structure and endowing with the ability to prevent volume shrinkage [22]. This can facilitate the dispersion of the active components of the catalyst in the course of the reaction, as well as improving mechanical strength and acid resistance, so as to increase the stability of catalysts [23]. Cu-based catalysts are highly active in CWPO [24], whereas there will be a leaching of the Cu species in the reaction [25,26]. Accordingly, by combining Ce oxide and CuO, Cu-Ce solid-melt catalyst was prepared, which might address the leaching problem of copper species. The fields of CO oxidation [27], N_2O catalytic decomposition [28], and toluene catalytic oxidation [29] etc. have reported Cu-Ce-O oxide catalysts. Yet no studies have been done on the use of Cu-Ce-O oxide catalysts for treatment of quinoline wastewater.

Following the complexation method, composite oxide catalysts with varying Cu/Ce molar ratios were prepared in this study. The catalyst prepared by the complexation method has high dispersion, and small particle size as compared with that prepared by other catalyst preparation methods [30]. Besides, the method makes Ce and Cu mix fully and form Cu-Ce oxide solid solution, thus increasing the catalytic performance. Given this, CWPO technology is adopted to degrade quinoline wastewater. The study of physical and chemical properties of different Cu/Ce molar catalysts has employed several characterization techniques, e.g. XRD, SEM, H_2-TPR and XPS to probe into the effects of different factors of the catalytic oxidation degradation performance of quinoline.

2. Experimental

2.1. Preparation of Ce-Cu mixed oxide catalysts

The complexation method was used to prepare Cu-Ce mixed oxide catalysts with CA (short for citric acid) serving as complexing agent. $Cu(NO_3)_2{\cdot}3H_2O$ and $Ce(NO_3)_3{\cdot}6H_2O$ with the Cu/Ce molar ratio of 1.0 were dissolved in distilled water in a typical preparation. A certain amount of CA was added into the solution to reach a 1.8 molar ratio of CA to (Ce + Cu). The mixture was then stirred to form a transparent solution. On that basis, the attained transparent solution was then evaporated to obtain solid powder, which was then treated at 80°C for 20 h. Afterwards, the dry powder was calcined at 650°C in a muffle furnace for 3.0 h to fabricate Cu_1Ce_1 mixed catalysts. The ramping rate of the muffle furnace reached 10°C min^{-1}. The Cu-Ce mixed oxide catalysts were marked as Cu_2Ce_1, Cu_1Ce_1, Cu_1Ce_2 and Cu_1Ce_3, respectively, following the corresponding Cu/Ce molar ratio of 2:1, 1:1, 1:2 and 1:3.The foregoing analytical reagents were purchased from Chengdu Kelong Chemical Reagent Factory.

2.2. Characterizations of Ce-Cu mixed oxide catalysts

The XRD studies of Cu-Ce mixed oxide catalysts were performed in the range of 2θ from 20 to 80°on a Rigaku XRD-6100 X-ray diffractometer, in which Cu Kα was line filtered by Ni. The tube voltage reached 40 kV, the tube current 30 mA, and the scanning rate 5° min^{-1}. The SEM images of Cu-Ce mixed oxide catalysts were captured using a Hitachi's S-4800 instrument. 30 mg of sample was placed in a U-shape quartz tube in each H_2-TPR test of Cu-Ce mixed oxide catalysts. The flow (25 mL min^{-1}) of 5.0% H_2-Ar mixture gas was controlled by a mass flow controller. The ramping rate reached 10°C min^{-1}. The chemical states of Ce, Cu and O catalysts were certified in the studied CeCu oxide using the XPS measurements. The signals were collected by employing a KRATOS X-ray sources (model XSAM800) with an aluminium crystal to generate the required Al Kα radiation, operating at 12 kV anode voltage and 12 mA emission current. The concentration of metal ions leached from Cu-Ce mixed oxide catalysts were tested by the AAS (short for atomic absorption spectrophotometer) on a Hitachi Z-5000 atomic absorption spectrophotometer. This study employed an ICP2060T inductively coupled plasma-optical emission spectroscopy (Jiangsu Skyray Instrument Co., Ltd.) to detect the initial copper and cerium content of the prepared catalytic materials, and the initial mole ratio of the

Cu_2Ce_1, Cu_1Ce_1, Cu_1Ce_2, and Cu_1Ce_3 catalysts are 1.98, 1.12, 0.49 and 0.28, respectively.

2.3. Catalytic tests of Ce-Cu mixed oxide catalysts

The CWPO reaction of quinoline containing wastewater was performed in a flask in a water bath. A certain amount of catalyst was added into the flask in a typical run, followed by the addition of quinoline containing wastewater (with initial pH value of 7.3) and hydrogen peroxide solution (30%). The reaction mixture was maintained in a water bath shaker at a constant temperature for a certain time. The centrifugal separation was then performed. For the detection of TOC value and catalytic activity, the supernatant fraction was extracted. The quinoline removal and H_2O_2 concentration (Titanium oxalate Spectrophotometric) in the CWPO of simulated quinoline containing wastewater were calculated with a Shimadzu UV-2550 UV-Vis (short for ultraviolet-visible spectrophotometer).The wavelength at 312.4 and 430 nm were established to respectively measure the absorbance of quinoline and H_2O_2 concentration. The catalytic activity was assessed by TOC (short for total organic carbon) with a TOC-VCPN Shimadzu TOC analyzer.

The catalytic activity was characterized by quinoline TOC removal "η" calculated with equation below:

$$\eta = \frac{c_0 - c_i}{c_0} \times 100\%$$

where η denotes the TOC removal; C_0 represents the TOC concentration of initial solution; C_i refers to the TOC concentration of the solution after reaction; the removal of quinoline oxidation and H_2O_2 conversion also refer to the foregoing formula.

3. Results and discussion

3.1. XRD Characterization

The XRD patterns of Cu-Ce-O composite oxide catalysts prepared with various Cu/Ce molar ratios after calcinations at 650°C are presented in Fig. 1. As shown in Fig. 1, the diffraction peaks of the crystallographic cubic CeO_2 crystalline phase [31] are identified at 2θ = 28.5° (111), 33.1° (200), 47.5° (220), 56.4° (311), 59.2° (222), 69.5° (400), 76.7 (331) and 79.1° (420), and crystalline phases of CuO are also observable through XRD at 2θ = 35.6° and 38.7°, respectively [32]. Some attained parameters are listed in Table 1 were analyzed and calculated after XRD data.

As the XRD in Fig. 1 suggests, the catalysts prepared at varying Cu/Ce molar ratios take on higher intensity CeO_2 crystal diffraction peaks and different intensities of CuO crystal diffraction peaks simultaneously. Besides, no splitting is to occur in the diffraction peaks. This suggests that $Ce(NO_3)_3{\cdot}6H_2O$ and $Cu(NO_3)_2{\cdot}3H_2O$ were decomposed at high temperature, and the Cu-Ce-O solid solution and CuO crystal phase were formed by the catalyst.

As Fig. 1 XRD presents, variations of CuO diffraction peak are obvious in the peak shape and peak intensity under varying molar ratios of Cu/Ce. When the molar ratio of Cu/Ce varies from small to large, the peak shape and peak intensity of CuO diffraction peak turn out to be narrower and stronger. As Table 1 lists, the grain size and crystallinity of CuO progressively enlarged. This means the phase structure of Cu-Ce-O composite oxide catalyst was largely impacted by the Cu/Ce molar ratio. This may consequently vary the content and structure of the active component Cu in the catalyst, thus decreasing the catalytic capacity.

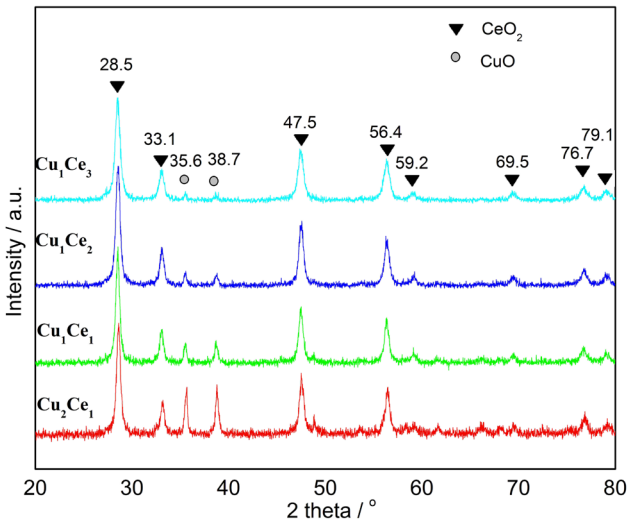

Fig. 1. XRD patterns of Cu-Ce-O composite oxide catalysts prepared under varying Cu/Ce molar ratios.

As Table 1 also lists, the Cu-Ce-O composite oxide catalyst is less than the pure phase CeO_2 unit in the *a* cell parameter (5.4103 Å). This suggests that Cu^{2+} with a small ionic radius is incorporated into the CeO_2 lattice under high temperature calcination, which makes CuO and CeO_2 interact with each other to produce a Cu-Ce-O solid solution. The formation of solid solution makes CuO and CeO_2 strongly interacted, which effectively weakens the Cu-O and Ce-O bond energy, making it easier to break in the reaction and generate a highly active oxygen species. Besides, the charge conversion effect of Cu^+/Cu^{2+} and Ce^{3+}/Ce^{4+} generated between CuO and CeO_2 can ensure transferring of electrons and oxygen ions and rapid regeneration [33] of the activity site in the catalytic system.

3.2. SEM analysis

Fig. 2 gives a SEM image of Cu-Ce-O composite oxide catalysts at varying Cu/Ce molar ratios prepared at high temperature calcination of 650°C. Fig. 2 illustrates the variation of pore size, particle size and uniformity on the surface of the catalyst at various Cu/Ce molar ratios, whereas numerous rough, loose and porous flocculent structures are formed, which is associated with the catalyst preparation method and high dispersibility of CeO_2. When the catalyst is being prepared, Cu^{2+} and Ce^{4+} are highly mixed under the complexation of citric acid. The volume is expanded after drying to form fluffy gel precursor in considerable amount, which is calcined at high temperature. Besides, CO_2, CO, H_2O and NO_x gases are produced in considerable amount as the citric acid and nitrate go through thermal decomposition. These gases are primarily attributed to the roughness, looseness and pore structure of the catalyst.

Table 1
Parameters of the catalysts prepared at different Cu/Ce molar ratios

Cu-Ce catalyst	Crystallinity (%)	Average crystallite size (nm)	Lattice parameters (a, $\alpha = 90°$, Å)	Lattice parameters (b, $\beta = 90°$, Å)	Lattice parameters (c, $\gamma = 90°$, Å)
Cu_2Ce_1	63.81	20.7	5.3988	5.4100	5.4003
Cu_1Ce_1	59.48	17.1	5.3996	5.4155	5.4088
Cu_1Ce_2	56.57	15.8	5.4031	5.4167	5.4085
Cu_1Ce_3	52.58	12.5	5.4097	5.4133	5.4081

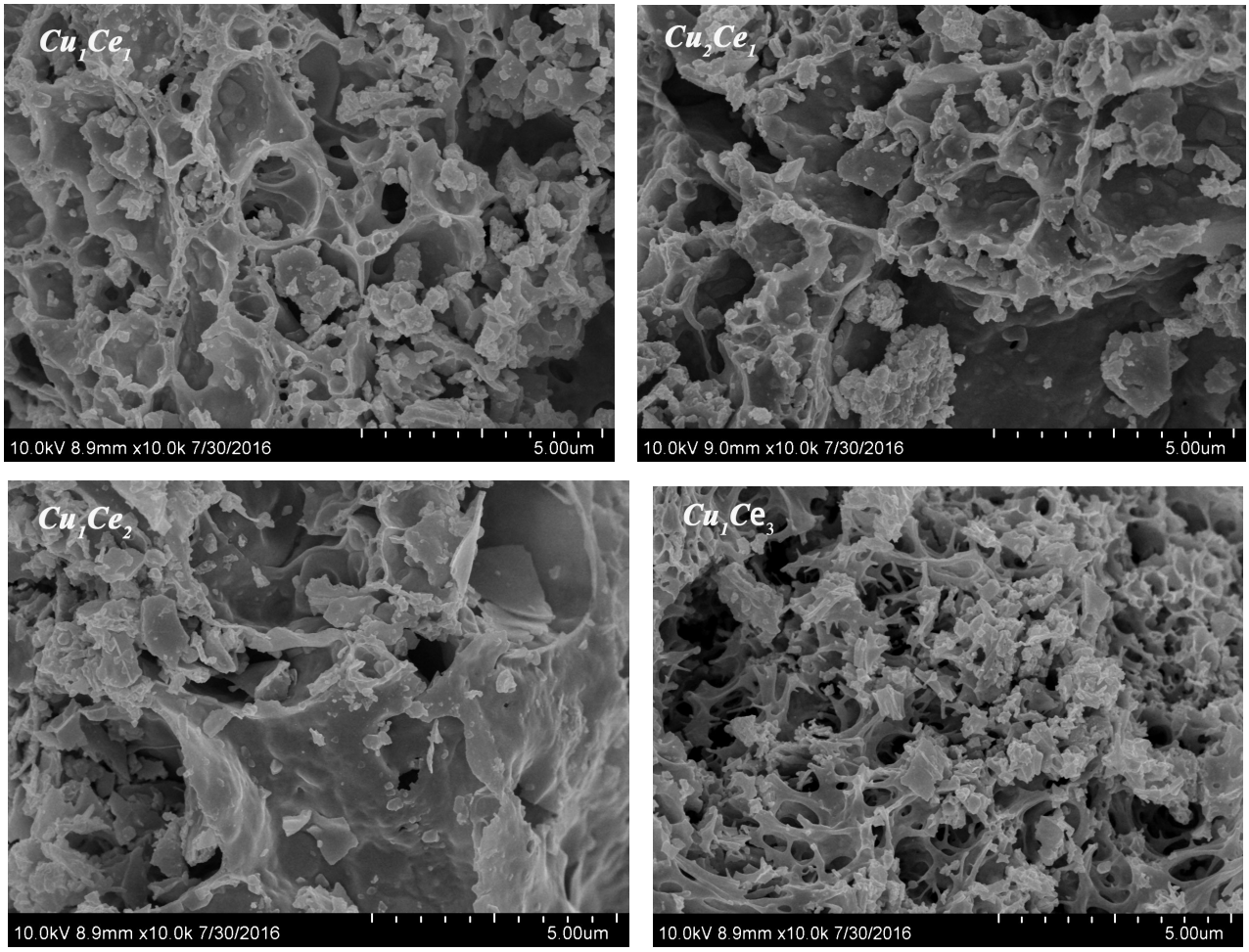

Fig. 2. SEM image of Cu-Ce-O composite oxide catalyst prepared at different Cu/Ce molar ratios.

As Fig. 2 presents, the Cu_2Ce_1 catalyst is evidently smalle than the Cu_1Ce_3 catalyst in pore structure and bulkiness, even though its surface is comparatively rough with plenty of bubbles and a porous structure. This is attributed to the incorporation of Ce, which effectively facilitates the dispersion of other metals on the carrier surface; when the Ce content is higher, it contributes more to the formation of pore structure and the improvement of its bulkiness. In this regard, it is conducive to increasing the full contact between the organic matter and the active component in the reaction and accelerating the oxidation and degradation of the organic matter.

3.3. H_2-TPR analysis

Fig. 3 presents the H_2-TPR spectra of the catalyst. As this figure presents, there were primarily two hydrogen consumption peaks. The α hydrogen consumption peak in Fig. 3 at the low temperature corresponding to 146, 153, 159 and 145 °C is formed by highly dispersed CuO on the catalyst surface and amorphous CuO with hydrogen consumption. The β hydrogen consumption peak at high temperatures corresponding to 231, 228, 220 and 206°C is formed by CuO in the catalyst body phase which strongly interacted with CeO_2 or CuO of larger particle formed after

agglomeration with hydrogen consumption [29,34]. Table 2 lists the results of the catalyst preparation under varying Cu/Ce molar ratios. The initial reaction temperature and the hydrogen consumption peak position are also different as this table presents. Yet the β hydrogen consumption peak moves obviously toward the high temperature direction as the Cu content increases, and the peak shape turns broadened, it will lead to the reducibility decreases. It is suggested that the content of CuO in the crystal phase of the catalyst surface or CuO of larger particle may increase as the copper content increases. As presented in XRD characterization data, the crystallite size and crystallinity increased, which moved the position of the hydrogen consumption peak to the high temperature direction.

Pure phase CeO_2 forms two H_2 hydrogen consumption peaks [35] at 500 and 800°C, respectively, as reported in the literature. The pure phase CuO forms a hydrogen consumption peak at approximately 300°C. As Fig. 3 suggests, the reduction temperature of the Cu-Ce-O composite oxide catalyst is apparently lower than the pure phase CeO_2 and CuO. This shows that the dispersion and self-properties of the CeO_2 and CuO species are varied in the Cu-Ce-O composite oxide catalyst. As the SEM analysis result suggests, the Cu-Ce-O composite oxide catalyst surface is a flocculent structure being rough and porous, which lays a solid foundation for the adsorption and reaction of H_2 molecules, thus promotes the reduction of surface reducible species. As XRD results indicate, Cu^{2+} with a smaller ion radius forms a Cu-Ce-O solid solution as dissolved in the CeO_2 lattice, which consequently shrinks the CeO_2 lattice, reduces the lattice constant and generates the lattice defects. Then, this Cu-Ce-O solid solution dissolution decreases the oxygen flow and notably increases its redox capacity, taking on potent low temperature reducibility.

3.4. XPS analysis

Fig. 4 gives the XPS spectra of the Cu-Ce-O composite oxide catalyst prepared under varying Cu/Ce molar ratios. As Fig. 4a presents, six intensive XPS peaks can be identified at 916.6, 907.1, 900.5, 898.9, 888.9 and 882.3 eV, respectively, in the Ce 3d XPS spectra of the Cu-Ce-O composite oxide catalysts. The peaks at 900.5 and 882.3 eV are attributed to the major peaks of Ce $3d_{3/2}$ and Ce $3d_{5/2}$, respectively. The peaks at 916.6, 907.1 and 898.9, 888.9 eV are satellite peaks of Ce $3d_{3/2}$ and Ce $3d_{5/2}$, respectively. As accordingly suggested, the Ce species in the catalysts primarily exist in four of the valence states, be speaking that the Ce species on the surface of the prepared catalyst primarily exist as a CeO_2 species [36,37]. This complies with the characterization result of XRD. As Fig. 4a presents, the electron binding energy values of the XPS peaks are consistent, suggesting that the valence and morphology of Ce species on the catalyst surface are basically the same, and not varied with Ce content variation.

As observed in Fig. 4b, the Cu 2p XPS spectra of the Cu-Ce-O composite oxide catalysts have four obvious XPS peaks at 961.6, 953.6, 941.8 and 933.6 eV, respectively. The peaks at 953.6 and 933.6 eV arise from the major peaks of Cu $2p_{1/2}$ and Cu $2p_{3/2}$, respectively. The peaks at 961.6 and 941.8 eV refer to the satellite peaks of Cu $2p_{1/2}$ and Cu $2p_{3/2}$, respectively. These four XPS peaks count as the characteristic peaks for Cu^{2+} species [38], which suggests that the Cu species on the surface of Cu-Ce-O composite oxide catalysts primarily exist as CuO. This complies with results of XRD characterization. The Cu/Ce molar ratio is different, and the intensity and peak area of Cu 2p XPS spectra notably differ from each other. The peak intensity and peak area of Cu 2p XPS increase progressively as the Cu/Ce molar ratio rises, which suggests the increase in the catalyst at the surface Cu^{2+} content. As Table 3 lists, the Cu content on the surface of the catalyst reaches the peak, and the content of Ce species is very low under the Cu/Ce molar ratio of 2. The Ce species content increased sharply, yet the content of Ce species decreased moderately as the Cu/Ce molar ratio decreased from 2 to 1. This suggests that the addition of Ce species would greatly impact the content of the Cu species at the catalyst surface.

A weak peak of Cu $2p_{3/2}$ at 932.4 eV is observable, which is attributed to the characteristic peak of Cu^{+} characteristic peak after the peak-splitting of Cu 2p XPS spectra from Fig. 4b [40]. While catalyst is under preparation, CO and other reducing gases generated through citric acid or thermal decomposition restore CuO species at high temperature; then, Cu_2O species are likely to occur in a small amount at the catalyst surface.

Fig. 4c gives the O 1s XPS spectra of the prepared Cu-Ce composite oxide catalyst. Three XPS peaks were acquired

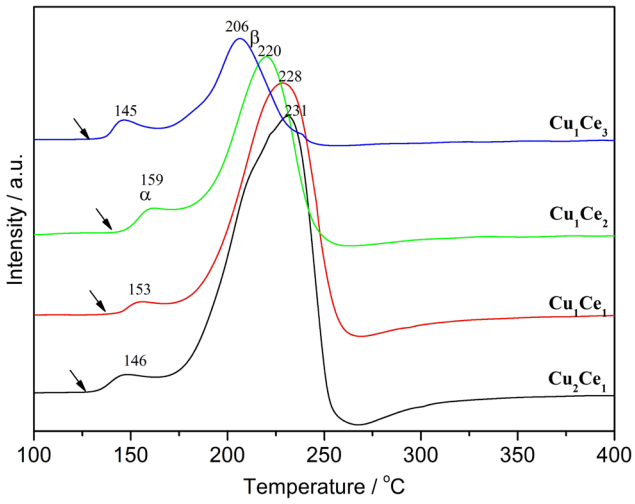

Fig. 3. Cu-Ce-O composite oxide catalysts before and after the reaction H_2 temperature reduction map.

Table 2
Catalyst baseline deviation and hydrogen consumption peak position data

CeCu catalysts	Initial reaction temperature (°C)	Hydrogen consumption peaks, α (°C)	Hydrogen consumption peaks, β (°C)
Cu_2Ce_1	129	146	231
Cu_1Ce_1	138	153	228
Cu_1Ce_2	136	159	220
Cu_1Ce_3	123	145	206

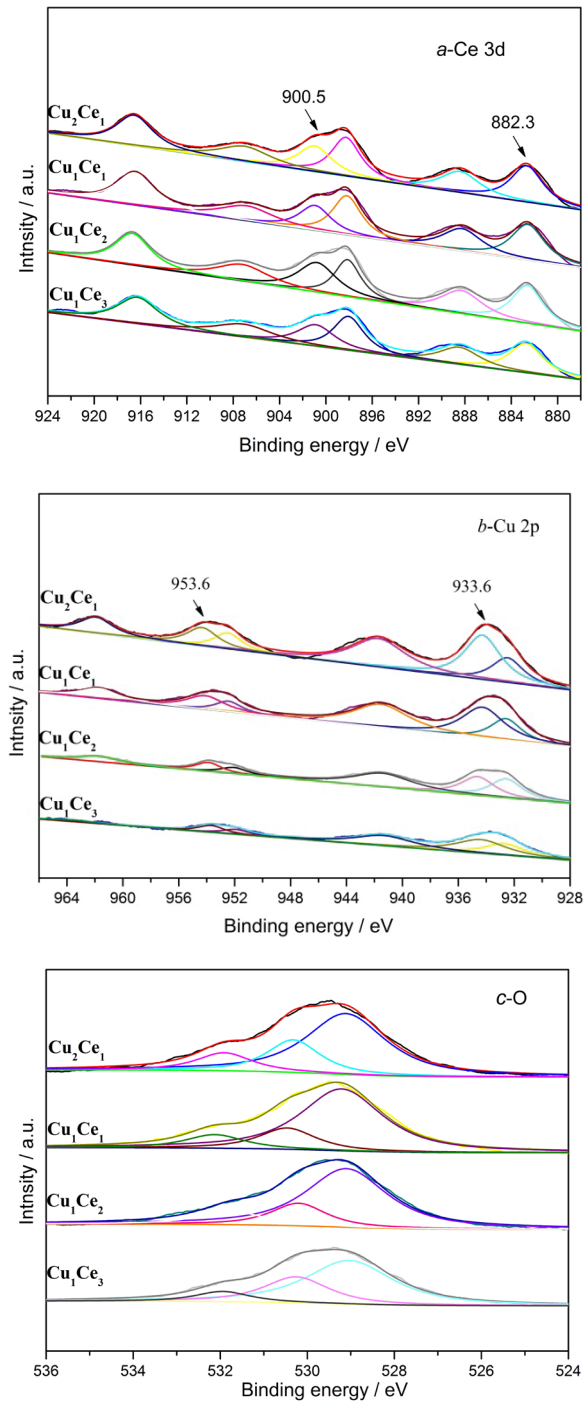

Fig. 4. Ce 3d, Cu 2p and O 1s XPS spectra of Cu-Ce-O composite oxide catalysts.

with an electron binding energy of 531.6, 530.3 and 529.2 eV, respectively,as peak separation of O 1s XPS spectrum was made. The electron binding energy of 529–530 eV arises from the surface of the catalyst lattice oxygen O^{2-},and the electron binding energy of 529.8-531 eV is attributed to the adsorption of oxygen O_2^{2-} or O^- on the surface of the catalyst; thus, the electron binding energy of 531.6 eV peak is hydroxyl OH^- [40,41] with surface water adsorption. As Fig. 4c presents, the catalyst lattice oxygen is greater than the adsorbed oxygen and hydroxyl oxygen in the XPS peak intensity and peak area. Table 3 lists that the content of lattice oxygen surmounts 62%, suggesting the surface is primarily encompassed by dispersed CuO, CeO_2 or Cu-Ce-O solid solution, which may be attributed to more oxygen vacancies formed by the interaction between CuO and CeO_2. Accordingly, the mobility and availability of lattice oxygen increased [42], and the doping of Ce contributes to the increase in the lattice oxygen content of the catalyst [43]. The lattice oxygen content is different as the Cu/Ce molar ratio is varying. As Table 3 lists, the lattice oxygen content is the highest under the molar ratio of Cu/Ce as 1, which may contribute to the catalytic reaction.

3.5. Effect of Cu/Ce molar ratio on catalytic activity

1 g $L^{-1}$of different Cu/Ce molar ratios catalyst,100 mg L^{-1} of simulated quinoline wastewater, and 196 mmol L^{-1} of 30% H_2O_2 were mixed in a reaction flask in each catalytic reaction test. The study measured the TOC removal at 75°C after 85 min of reaction. The results are presented in Fig. 5. As this figure presents, the TOC removal rapidly increases with the increase of molar ratio as the molar ratio of Cu/Ce is below 1.0. The TOC removal decreases with the increase of the molar ratio as the molar ratio of Cu/Ce surmounts 1.0. The Cu-Ce-O composite oxide catalyst takes on the optimal catalytic activity, and the TOC removal reaches 88.4% under the molar ratio of Cu/Ce as 1.0.

As the experimental results present, the adsorption, volatilization and H_2O_2 oxidation of catalyst contribute less to the TOC removal under the identical reaction conditions with merely 6.3%, 6.6% and 5.9% removed 85 min after the reaction. As accordingly indicated, catalytic oxidation is dominated in the removal of quinoline.

The catalytic performance of the catalyst has a certain relationship with its active components and structure in the quinoline CWPO reaction. The catalyst, as incorporated by XRD and XPS characterization, primarily forms a Cu-Ce-O solid, presenting Ce^{4+}, Cu^{2+} and rich O Species on the surface. In Cu-Ce-O solid solution, Cu^{2+} substituted CeO_2 lattice in the part of Ce^{4+} and destroyed the coordination of CeO_2 lattice balance, in which gave rise to the oxygen vacancies. Such vacancies better increase the catalyst adsorption of oxygen molecules and activation ability, and also contribute to the oxygen species in the catalyst diffusion and migration. As a result, this makes the active oxygen species more convenient to move to the catalyst surface and increases the catalyst surface oxidation performance. Also, a strong interaction force is established between CuO and CeO_2 arising from the formation of the solidified solution, which drops the reaction temperature, and increases the reactivity and the structural stability of the catalyst. The relative content of Cu species in the catalyst decreases under the low molar ratio of Cu/Ce. As XPS results suggest, Cu_1Ce_3 catalyst merely has 8.92% Cu, and the lowest content of lattice oxygen reaches 62.71%. This suggests that such catalyst does not contribute to the formation of solid solution.

When the molar ratio of Cu/Ce is high, a large amount of Cu species cannot be well dissolved in the CeO_2 lattice,

Table 3
Results of XPS analysis of Cu-Ce-O composite oxide catalyst

CeCu catalysts	Lattice oxygen (%)	Adsorbed oxygen (%)	Hydroxyl oxygen (%)	Ce (at%)	Cu (at%)	O (at%)
Cu_2Ce_1	64.10	22.75	13.14	2.44	18.90	78.67
Cu_1Ce_1	71.67	17.09	11.24	21.43	13.06	65.51
Cu_1Ce_2	69.16	18.07	12.77	25.22	8.49	66.30
Cu_1Ce_3	62.71	28.04	9.25	23.68	8.92	67.39

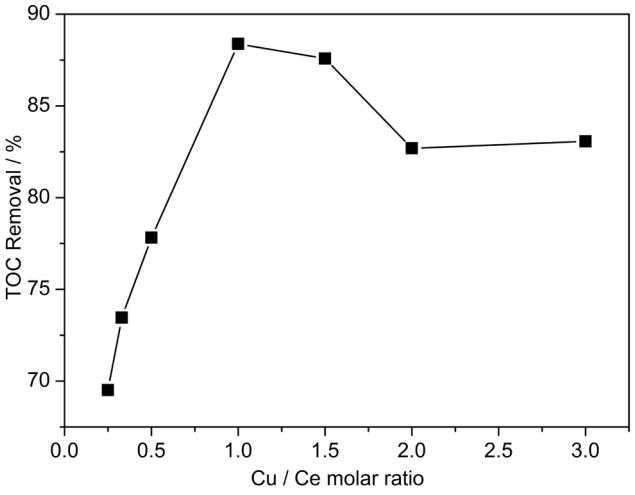

Fig. 5. Effect of Cu/Ce molar ratio on catalytic activity with: 100 mg L^{-1} wastewater, 1 g L^{-1} catalyst, 196 mmol L^{-1} H_2O_2, 85 min, 75°C and pH 7.3.

while the CuO is formed on the surface of the catalyst, e.g. Cu_2Ce_1, the surface Cu content is the highest, which is 18.90%, whereas the lattice oxygen content is merely 64.10%. This is probably because the CuO content in the catalyst surmounts the saturated capacity of the CeO_2 lattice, and numerous CuO fails to be fully dissolved in the CeO_2 lattice or well interacted with CeO_2. This readily loses the active Cu components. Thus, the interaction between the Cu species and the Ce species will be weakened by either too high or too low Cu/Ce molar ratios, taking on poor catalytic activity. The TOC removal reaches the peak under the molar ratio of Cu/Ce as 1.0. This is probably because the Cu species can be well dissolved in the CeO_2 lattice to form a solidified solution at this molar ratio, and have numerous active sites, making it easier to activate H_2O_2 molecules in the catalytic reaction.

3.6. Effect of catalyst dosage on catalytic activity

In each catalytic reaction test, different mass of Cu/Ce at molar ratio of 1.0, 100 mg L^{-1} of simulated quinoline wastewater, 196 mmol L^{-1} of 30% H_2O_2 were mixed in a reaction flask. The reaction was conducted at 75°C for 85 min. The results are shown in Fig. 6. As presented in Fig. 6, when the amount of catalyst increased from 0.04 g L^{-1} to 0.16 g L^{-1}, the TOC removal increased rapidly from 16.6%

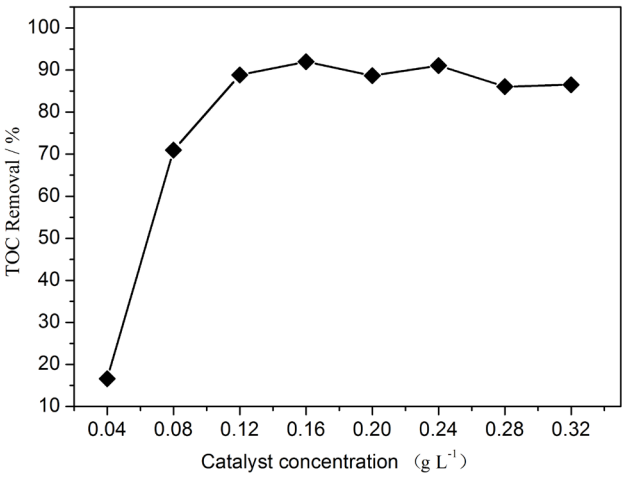

Fig. 6. Effect of catalyst dosage on catalytic activity with: 100 mg L^{-1} wastewater, 196 mmol L^{-1} H_2O_2, 85 min, 75°C and pH 7.3.

to 91.1%. When the amount of catalyst is more than 0.16 g L^{-1}, the TOC removal curve of quinoline reaches a plateau.

When the catalyst is small in dosage, the catalyst active centers are small in amount under the identical conditions; in the meantime, ·OH species taking on potent oxidizing properties generated by activating H_2O_2 molecules is less, which consequently decreases the TOC removal of Quinoline. The amount of active centers provided by the catalyst to the reaction system increases greatly as the amount of catalyst is increased. This greatly rises the content of ·OH species in the solution and degrades quinoline rapidly. As catalysts are excessively used, the decomposition of H_2O_2 molecules will be accelerated, and the effective utilization ratio of H_2O_2 will decrease, thus decreasing the removal of TOC.

3.7. The effect of H_2O_2 dosage on the catalytic activity

1 g L^{-1} of Cu/Ce at molar ratio of 1.0,100 mg $L^{-1}$of simulated quinoline wastewater, and different mmol L^{-1} of 30% H_2O_2 were mixed in a reaction flask in each catalytic reaction test. At 75°C reaction temperature, the TOC removal was measured in different reaction times. The impact of H_2O_2 dosage on the catalytic activity of quinoline was ascertained by 2 (39 mmol L^{-1}), 6 (118 mmol L^{-1}) and 10 (196 mmol L^{-1}) times the stoichiometric value, respectively. The results are presented in Fig. 7.

As Fig. 7 suggests, the TOC removal increased notably as H_2O_2 dosage increased. TheTOC removal increased from 8.8 to 90.6% at 35 min when the dosage of H_2O_2 increased from 2 times (39 mmol L^{-1}) to 10 times (196 mmol L^{-1}). When the dosage of H_2O_2continued to increase, the TOC removal curve of quinoline tended to be straight. The TOC removal was lower with the reaction time under the H_2O_2 dosage of 2 times. This is because the active oxidizing species ·OH provided by H_2O_2 in the reaction system was low in amount, which means the quinoline could not be effectively oxidized and degraded. The TOC removal after reaction 35 min was 86.6 and 90.6%, respectively, as the H_2O_2 dosage was 6 and 10 times. The amount of ·OH oxidizing species

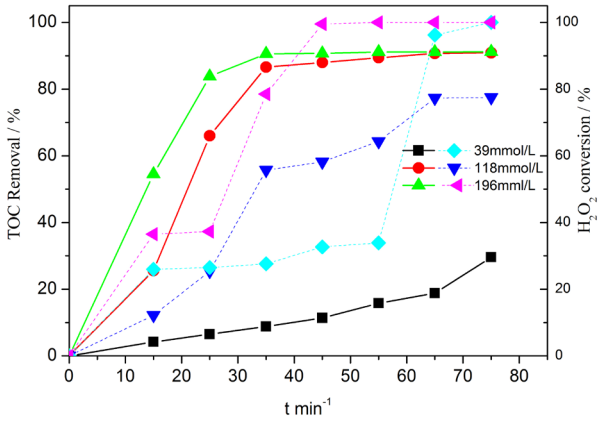

Fig. 7. Effect of H_2O_2 dosages on the catalytic activity with: 100 mg L^{-1} wastewater, 1 g L^{-1} catalyst, 75°C and pH 7.3. Solid line stands for TOC removal while dashed for H_2O_2 conversion.

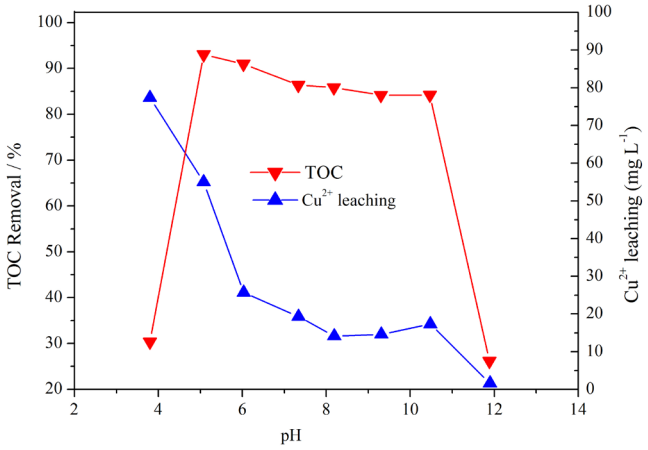

Fig. 8. Effect of initial pH on catalytic activity with: 100 mg L^{-1} wastewater, 1 g L^{-1} catalyst, 196 mmol L^{-1} H_2O_2, 85 min and 75°C.

formed in the reaction system greatly increased, and the sufficient reaction of ·OH with quinoline facilitated the oxidative degradation of quinoline as H_2O_2 dosage increased. Accordingly, the excessive dosage of H_2O_2 is conducive to the rapid oxidative degradation of quinoline.

The consumption of H_2O_2 accelerated as H_2O_2 dosage increased. This may be attributed to the formation of numerous ·OH involved in the reaction or to the side effects of H_2O_2, e.g. H_2O_2 thermal decomposition. Besides, the ·OH generated will produce their own consumption reaction, which will produce weak oxidation species (inclusive of HO_2 and O_2) [44].

3.8. Effect of initial pH value on the quinoline catalytic activity and the stability of catalyst

1 g L^{-1} of Cu/Ce at molar ratio of 1.0, 100 mg L^{-1} of simulated quinoline wastewater, 196 mmol L^{-1} of 30% H_2O_2 were mixed in a reaction flask in each catalytic reaction test. The reaction was performed at 75°C for 85 min. The results are presented in Fig. 8.

As Fig. 8 presents, the TOC removal is 30.4%under the pH value of the reaction system as 3.8; the TOC removal sharply increases to 93.0%under the pH value of the reaction system as 5.1; the TOC removal is more than 84.1%, and the change range is not significant under the pH value of the system as 5.1–10.5; the TOC removal declines sharply to 26.2% under the pH value of the reaction system as 11.9. This suggests that the pH value of the reaction system notably impacts the TOC removal. The Cu-Ce-O oxide catalyst is also observed with good pH adaptability in quinoline CWPO reaction. As Fig. 8 presents, the stability of the catalyst, namely the leaching concentration of Cu^{2+}, is largely associated with the pH value, and its tendency is to decrease as pH value increases; thus, the leaching of Cu^{2+} reaches 77.32 mg L^{-1}, under the reaction system pH of 3.8, and the minimum of leaching of Cu^{2+}reaches14.16 mg L^{-1} at pH 8.19. Accordingly, the stability of the catalyst is revealed here as strongly associated with the pH value of the solution in quinoline CWPO.

The TOC removal is comparatively low under the relatively low pH value of the reaction system. This is probably because: on the one hand, the catalyst part of the Cu-Ce-O solid solution structure is destroyed as the CuO species in the catalyst are dissolved under acidic conditions, making the number of catalyst center surface activities decline. This is not conducive to activating H_2O_2 molecules. On the other hand, the slow decomposition of H_2O_2 under acidic conditions may decrease the level of H_2O_2 decomposition rate to generate ·OH. The TOC removal decreases sharply when the pH value of the reaction system is above 11.9. This is because H_2O_2 reacts with ·OH and produces HO_2· and O_2 at higher pH, resulting in sharp decline in the amount of ·OH, which is not conducive to oxidizing quinoline transformation.

The Cu-Ce-O oxide catalyst is highly adaptable to pH, which is probably attributed to the addition of rare earth element Ce. The addition of Ce can disperse and stabilize the active components in the catalyst. The formation of Cu-Ce-O solid solution in this catalyst system will produce a strong interaction between CuO and CeO_2, which is conducive to reducing the precipitation of Cu^{2+}.

3.9. Kinetics study

This study started with four steps: 1), Add 1 g L^{-1} of catalyst, with a Cu/Ce molar ratio of 1.0, to 100 mL of quinoline simulated wastewater with a concentration of 100 mg L^{-1}; 2), add 196 mmol L^{-1} of H_2O_2 to the reaction flask, and 3), test the quinoline oxidation conversion at different temperatures of 55, 65, 75 and 85°C and 4), and study its kinetics. Since the experiment was performed under the condition that the reaction conditions remained consistent, and the oxidation transformation of quinoline was assumed consistent with the quasi-first order kinetic model equation. The results are presented in Figs. 9 and 10. The specific kinetic parameters are listed in Table 4.

As Fig. 9 presents, the reaction temperatures were 55, 65, 75 and 85°C, and the reaction rates were 0.015, 0.031, 0.054 and 0.131 min^{-1}, respectively. As this figure also presents, the reaction rate varied slightly at 55 and 65°C but significantly at 55 and 85°C. This suggests that the removal of quinoline at a certain temperature increased as the reaction temperature rose. This may be attributed to the natural ability of higher temperatures to expedite the activation of

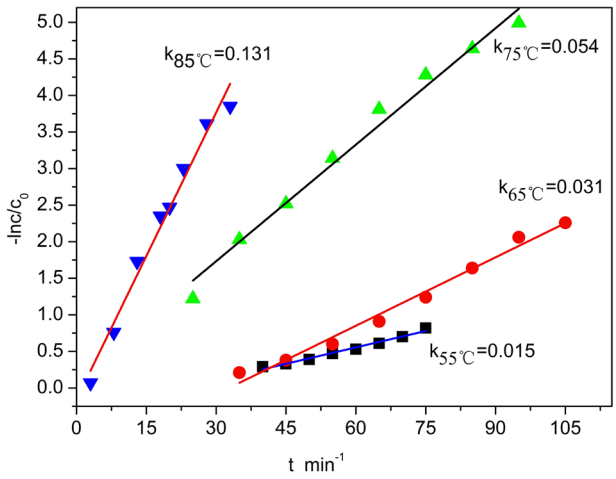

Fig. 9. The constants for quinoline removal kinetics under different conditions: 100 mg L^{-1} wastewater, 1 g L^{-1} of catalyst, 196 mmol L^{-1} H_2O_2 and pH 7.3.

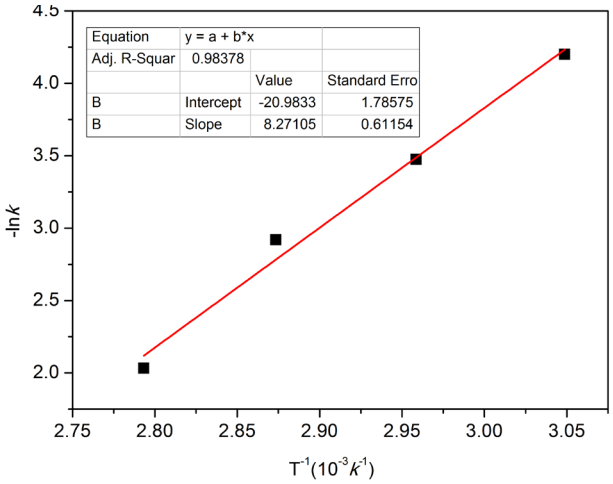

Fig. 10. Relationship of –ln$k$ and T^{-1} in different temperature: 100 mg L^{-1} wastewater, 1 g L^{-1} of catalyst, 196 mmol L^{-1} H_2O_2 and pH 7.3.

Table 4
Kinetic parameters of quinoline removal reaction under different reaction temperatures

T°C	First order reaction kinetics equation	k (min^{-1})	R^2	Ea (kJ mol^{-1})
55	$\ln(C_t/C_0) = -0.015x + 0.344$	0.015	0.981	68.766
65	$\ln(C_t/C_0) = -0.031x + 1.022$	0.031	0.986	
75	$\ln(C_t/C_0) = -0.054x - 0.090$	0.054	0.986	
85	$\ln(C_t/C_0) = -0.131x + 0.157$	0.131	0.981	

H_2O_2 into ·OH in the reaction system. The catalytic induction period can be shortened simultaneously, and the high temperature also offers higher external energy to the reaction,enabling it to rapidly reach the energy activation state for quinoline catalytic degradation.

As shown in Table 4, the correlation coefficient R^2 at the reaction temperature of 55, 65, 75 and 85°C is 0.981, 0.986, 0.986 and 0.981, respectively, under the wavelength of 312.4 nm, showing a potent linear relationship. This suggests the CWPO reaction to oxidation of quinoline complies with the quasi-first order reaction kinetics equation. As shown in Fig. 10, the relationship between –ln$K$ and $1/T$ is linear. Its linear correlation coefficient (R^2) is 0.9892, indicating a good linear relationship. In the equation: –ln$K$ = –ln$A$ + E/RT, which was drawn in Fig. 10, its slope is E/R and intercept-ln$A$. The activation energy calculated in this study using the slope is 68.766 kJ/mol.

4. Conclusions

Following a citric acid-aided complexation method, the Cu-Ce composite oxide catalysts were prepared. By dissolving Cu species into the CeO_2 lattice at high temperatures, a Cu-Ce-O solid solution was formed. As citric acid and nitric acid were decomposed, gas was produced in considerable amount, and the surface of catalyst took on a loose and porous structure. As the XPS characterization suggests, CeO_2 and CuO species are mainly present on the surface of the catalyst, which might also involve Cu_2O in a small amount. The surface lattice oxygen content is greater than the adsorbed oxygen and hydroxyl oxygen. The phase structure of the Cu-Ce composite oxide catalysts were largely impacted by the molar ratio of Cu/Ce. The peak shape and peak intensity of the CuO diffraction peak turn stronger, and the reducibility decreases as Cu content increases.

The prepared Cu-Ce composite oxide catalyst takes on potent CWPO performance for simulated quinoline wastewater. The catalyst takes on the optimal catalytic activity under the catalyst Cu/Ce molar ratio of 1.0. As the amount of catalyst and H_2O_2 increases, the TOC removal increases rapidly. Yet when it increases to a certain extent, the removal curve turns out to be gentle. The TOC removal is comparatively low, under the lower or higher initial pH of the solution. And the TOC removal is comparatively high at pH 5.1–10.5. The stability of the catalyst, i.e. the concentration of Cu^{2+}, will decrease as pH increases. The catalyst complies with the quasi-first order reaction kinetics equation in the CWPO reaction degradation of Quinoline. The removal of TOC is up to 91.1%under the molar ratio of Cu/Ce as 1.0 and the amount of the catalyst and H_2O_2 as 0.16 g L^{-1} and 196 mmol L^{-1}, respectively. The preparation of the catalyst and adopting CWPO technology in the degradation of quinoline provides a reference solution for the treatment of refractory wastewater.

Acknowledgements

This work is supported by the Key Special Project of Strategic International Scientific and Technological Innovation Cooperation (2016YFE0205600), Project of National Natural Science Foundation of China (21676037, B061201, 51408215), the Project of Scientific and Technological Research Program of Chongqing Municipal Education Commission (KJ120720), the Project of Chongqing Technology and Business University of Young Doctor Foundation

(1352023) and the Project of Research Program of Chongqing Science and Technology Commission (cstc2015shmsztzx20001, cstc2017jcyjAX0192).

References

[1] A. Rubio-Clemente, R.A. Torres-Palma, G.A. Peñuela, Removal of polycyclic aromatic hydrocarbons in aqueous environment by chemical treatments: A review, Sci. Total Environ., 478 (2014) 201–225.

[2] C. Wang, K. Ma, T. Wu, M. Ye, P. Tan, K. Yan, Electrochemical mineralization pathway of quinoline by boron-doped diamond anodes, Chemosphere, 149 (2016) 219–223.

[3] S. Meyer, S. Cartellieri, H. Steinhart, Simultaneous determination of PAHs, hetero-PAHs (N, S, O), and their degradation products in creosote-contaminated soils. method development, validation, and application to hazardous waste sites, Anal. Chem., 71 (1999) 4023–4029.

[4] D. Rameshrajaa, V.C. Srivastavaa, J.P. Kushwahab, I.D. Malla, Quinoline adsorption onto granular activated carbon and bagasse fly ash, Chem. Eng. J., 181–182 (2012) 343– 351.

[5] B.U. Bohlmann, M. Bohnet, Improvement of process stability of microbiological quinoline degradation in a three-phase fluidized bed reactor, Chem. Eng. Technol., 2 (2001) 91–96.

[6] I. Weid, J.M. Marques, C.D. Cunha, R.K. Lippi, S.C.C. dos Santos, A.S. Rosado, U. Lins, L. Seldin, Identification and biodegradation potential of a novel strain of dietzia cinnamea isolated from a petroleum-contaminated tropical soil, Syst. Appl. Microbial., 30 (2007) 331–339.

[7] K. Sugaya, O. Nakayama, N. Hinata, K. Kamekura, A. Ito, Biodegradation of quinoline in crude oil, J. Chem. Technol. Biotechnol., 76 (2010) 603–611.

[8] L. Sun, B. Tuo, Q. Wang, J. Yan, Study on the isolation of bacteria for quinoline degradation and enhanced treatment of refining wastewater, Pet. Process Petroche., 43 (2012) 71–75.

[9] P. Zhang, X. Zhang, Y. Fang, Y. Lan, Adsorption characteristics of quinoline on activated carbon fiber, Chem. Ind. Eng. Prog., 32 (2013) 209–213.

[10] L.DS. Pinto, L.M.F. Santos, B. Al-Duri1, R.CD. Santos, Supercritical water oxidation of quinoline in a continuous plug flow reactor-part 1: effect of key operating parameters, J. Chem. Technol. Biotechnol., 81 (2006) 912–918.

[11] A. Chen, L. Zhang, F. Chang, Y. Ge, K. Wang, Degradation of quinoline from biotreated effluent with ozone-based advanced oxidation processes, Chinese J. Environ. Eng., 9 (2015) 5795–5800.

[12] D.R. Stapleton, I.K. Konstantinou, A. Karakitsou, D.G. Hela, M. Papadaki, 2-Hydroxypyridine photolytic degradation by 254nm UV irradiation at different conditions, Chemosphere, 77 (2009) 1099–1105.

[13] R. Enriquez, P. Pichat, Interactions of humic acid, quinoline, and TiO_2 in water in relation to quinoline photocatalytic removal, Langmuir, 17 (2001) 6132–6137.

[14] X. Xing, X. Zhu, H. Li, Y. Jiang, J. Ni, Electrochemical oxidation of nitrogen-heterocyclic compounds at boron-doped diamond electrode, Chemosphere, 86 (2012) 368–375.

[15] A.B. Thomsen, F. Laturnus, The influence of different soil constituents on the reaction kinetics of wet oxidation of the creosote compound quinoline, J. Hazard. Mater., 81 (2001) 193–203.

[16] S. Navalon, M. Alvaro, H. Garcia, Heterogeneous fenton catalysts based on clays, silicas and zeolites, Appl. Catal., B, 99 (2010) 1–26.

[17] M. Kurian, D.S. Nair, A.M. Rahnamol, Influence of the synthesis conditions on the catalytic efficiency of $NiFe_2O_4$ and $ZnFe_2O_4$ nanoparticles towards the wet peroxide oxidation of 4-chlorophenol, React. Kinet. Catal. Lett., 111 (2014) 591–604.

[18] M. Kurian, C. Kunjachan, A. Sreevalsan, Catalytic degradation of chlorinated organic pollutants over $Ce_xFe_{1-x}O_2$ (x: 0, 0.25, 0.5, 0.75, 1) nanocomposites at mild conditions, Chem. Eng. J., 308 (2017) 67–77.

[19] W. Wang, Q. Zhu, F. Qin, Q.G. Dai, X.Y. Wang, Fe doped CeO_2 nanosheets as fenton-like heterogeneous catalysts for degradation of salicylic acid, Chem. Eng. J., 333 (2018) 226–239.

[20] G. Lafaye, J.B. Jr., D. Duprez, Impact of cerium-based support oxides in catalytic wet air oxidation: conflicting role of redox and acid-base properties, Catal. Today, 253 (2015) 89–98.

[21] A.M.T. Silva, R.R.N. Marques, R.M. Quinta-Ferreira, Catalysts based in cerium oxide for wet oxidation of acrylic acid in the prevention of environmental risks, Appl. Catal., B, 47 (2004) 269–279.

[22] S. Mnasri-Ghnimi, N. Frini-Srasra, Catalytic wet peroxide oxidation of phenol over Ce-Zr-modified clays: effect of the pillaring method, Korean J. Chem. Eng., 32 (2015) 68–73.

[23] A. Trovarelli, C.D. Leitenburg, M. Boaro, G. Dolcetti, The utilization of ceria in industrial catalysis, Catal. Today, 50 (1999) 353–367.

[24] J. Han, H.Y. Zeng, S. Xu, C.R. Chen, X.J. Liu, Catalytic properties of CuMgAlO catalyst and degradation mechanismin CWPO of methyl orange, Appl. Catal., A, 527 (2016) 72–80.

[25] S.S. Jiang, H.P. Zhang, Y. Yan, Cu-MFI zeolite supported on paper-like sintered stainless fiber for catalytic wet peroxide oxidation of phenol in a batch reactor, Sep. Purif. Technol., 90 (2018) 243–251.

[26] N. Inchaurrondo, J. Cechini, J. Font, P. Haure, Strategies for enhanced CWPO of phenol solutions, Appl. Catal., B, 111–112 (2012) 641–648.

[27] W. Liu, M. Flytzani-Stephanopoulos, Total oxidation of carbon monoxide and methane over transition metal fluorite oxide composite Catalysts: II. catalyst characterization and reaction-kinetics, J. Catal., 153 (1995) 317–332.

[28] Z. Liu, C. He, B. Chen, H. Liu, CuO-CeO_2 mixed oxide catalyst for the catalytic decomposition of N_2O in the presence of oxygen, Catal. Today, 5 (2017) 1–6.

[29] G. Zhou, H. Lan, T. Gao, H. Xie, Influence of Ce/Cu ratio on the performance of ordered mesoporous CeCu composite oxide catalysts, Chem. Eng. J., 246 (2014) 53–63.

[30] L. Shi, C.Y. Zeng, Q.H. Lin, P. Lu, W.Q. Niu, N. Tsubakib, Citric acid assisted one-step synthesis of highly dispersed metallic Co/SiO_2 without further reduction: As-prepared Co/SiO_2 catalysts for Fischer-Tropsch synthesis, Catal. Today, 228 (2014) 206–211.

[31] X. Yang, F. Meng, G. Chen, X. Zhang, Synthesis and microstructures characterization of trigonometry-star-like CeO_2, J. Synth. Cryst., 44 (2015) 44:3612.

[32] Y. Li, C. Wang, G. Liu, L. Zeng, Y. He, J. Zeng, Influence of additives on structure and performance of CeO_2-ZrO_2-Al_2O_3 composite oxide, Chin. J. Nonferrous. Met., 26 (2016) 1255–1263.

[33] U. Menon, H. Poelman, V. Bliznuk, V.V. Galvita, D. Poelman, G.B. Marin, Nature of the active sites for the total oxidation of toluene by $CuOCeO_2/Al_2O_3$, J. Catal., 295 (2012) 91–103.

[34] H. Xie, Q. Du, H. Li, G. Zhou, S. Chen, Z. Jiao, J. Ren, Catalytic combustion of volatile aromatic compounds over CuO-CeO_2 catalyst, Korean J. Chem. Eng., 34 (2017) 1944–1951.

[35] H.C. Yao, Y.F.Y. Yao, Ceria in automotive exhaust catalysts: I. oxygen storage, J. Catal., 86 (1984) 254–265.

[36] C. He, Y. Yu, C. Chen, L. Yue, N. Qiao, Q. Shen, J. Chen, Z. Hao, Facile preparation of 3D ordered mesoporous CuO_x-CeO_2 with notably enhanced efficiency for the low temperature oxidation of heteroatom-containing volatile organic compounds, RSC Adv., 3 (2013) 19639–19656.

[37] J. Fan, X. Wu, X. Wu, Q. Liang, R. Ran, D. Weng, Thermal ageing of Pt on low-surface-area CeO_2-ZrO_2-La_2O_3 mixed oxides: effect on the OSC performance, Appl. Catal., B, 81 (2008) 38–48.

[38] J. Zhu, Q. Gao, Z. Chen, Preparation of mesoporous copper cerium bimetal oxides with high performance for catalytic oxidation of carbon monoxide, Appl. Catal., B, 81 (2008) 236–243.

[39] S. Zeng, Y. Wang, K. Liu, F. Liu, H. Su, CeO_2 nanoparticles supported on CuO with petal-like and sphere-flower morphologies for preferential CO oxidation, Int. J. Hydrogen Energy, 37 (2012) 11640–11649.

[40] Z. Song, P. Ning, Q. Zhang, X. Liu, J. Zhang, Y. Wang, Y. Duan, Z. Huang, The role of surface properties of silicotungstic acid doped CeO_2 for selective catalytic reduction of NOx by NH_3: effect of precipitant, J. Mol. Catal. A: Chem.: Chemical, 413 (2016) 15–23.
[41] L. Jiang, H. Zhu, R. Razzaq, M. Zhu, C. Li, Z. Li, Effect of zirconium addition on the structure and properties of CuO/CeO_2 catalysts for high-temperature water-gas shift in an IGCC system, Int. J. Hydrogen Energy, 37 (2012) 15914–15924.
[42] Q. Dai, H. Huang, Y. Zhu, W. Deng, S. Bai, X. Wang, G. Lu, Catalysis oxidation of 1,2-dichloroethane and ethylacetate over ceria nanocrystals with well-defined crystal planes, Appl. Catal., B, 117–118 (2012) 360–368.
[43] M. Sun, L. Yu, J. Yu, Q. Yu, Z. Hao, Catalytic combustion of dimethyl ether over Ce-doped cryptomelane type manganese oxide, J. Fuel Chem. Technol., 38 (2010) 108–115.
[44] M. Huang, C. Xu, Z. Wu, Y. Huang, J. Lin, J. Wu, Photocatalytic discolorization of methyl orange solution by Pt modified TiO_2 loaded on natural zeolite, Dyes Pigments, 77 (2008) 327–334.